BIOCELL
2020 44(3): 389-400

Tech Science Press

Enhanced osteogenic differentiation of human periodontal ligament stem cells by suberoylanilide hydroxamic acid

Yunze XUAN[1,#]; Bin JIN[1,#]; Sayan Deb DUTTA[5,#]; Mengmeng LIU[2]; Zaixian SHEN[1]; Xiwen LIU[3]; Yang KANGJUAN[4,*]; Lim KI-TAEK[5,*]

[1] Department of Stomatology, Affiliated Hospital of Yanbian University, Yanji, 133000, China
[2] Department of Immunology and Molecular Microbiology, School of Dentistry and Dental Research Institute, Seoul National University, Seoul, 08826, South Korea
[3] Affiliated Hospital of Yanbian University, Yanji, 133000, China
[4] Department of Cell Biology and Medical Genetics, Yanbian University Medical College, Yanji, 133000, China
[5] Department of Biosystems Engineering, Kangwon National University, Chuncheon, 24341, South Korea

Key words: Suberoylanilide hydroxamic acid, Histone deacetylase, Osteoblast, hPDLSCs, Alkaline phosphatase, Periodontal bone regeneration

Abstract: Periodontitis is a type of chronic inflammation in the gingival tissue caused by infectious bacteria colonizing the surface of the teeth, leading to the destruction of tooth-supporting tissues and loss of alveolar bone. Suberoylanilide hydroxamic acid (SAHA), a class of histone deacetylase (HDAC) inhibitor, has the potential to stimulate osteoblast differentiation by acetylating histone proteins, and thus suppressing the expression of adipogenic and chondrogenic genes. However, the effect of SAHA on the differentiation of human periodontal ligament stem cells (hPDLSCs) is yet to be elucidated. Herein, we investigated the effects of SAHA on *in vitro* proliferation and differentiation of hPDLSCs by MTT assay, Alizarin Red-S, and alkaline phosphatase staining, and real-time PCR. Notably, 300 ng/mL SAHA treatment enhanced the proliferation and mineralization of hPDLSCs, indicating their osteogenic potential. Moreover, a significant enhancement of osteogenesis gene markers and proteins was observed. We also demonstrated that ERK is a positive regulator of Runx2 transcription factors during osteoblast differentiation. These results indicate that SAHA may be a useful osteogenic induction agent for periodontal bone regeneration.

Introduction

Periodontitis is a destructive inflammation in the surrounding and supporting structures of the teeth that results in tissue injury, including loss of connective tissue and alveolar bone (Straka *et al.*, 2015; Larsson *et al.*, 2015). Consequently, periodontitis often leads to loose teeth and is the primary cause of tooth loss. At present, more and more scientists are focusing on tissue reconstruction, and strive to preserve physiologically functional teeth in the mouth for an extended period of time. In recent years, the potential application of mesenchymal stem cells (MSCs) for tissue regeneration has attracted much attention in various medical studies. It is reported that there are abundant mesenchymal stem cell pools in the oral cavity (Huang *et al.*, 2009). Human dental pulp mesenchymal stem cells (hDMSCs) can be isolated in the form of dental pulp stem cells (DPSCs), periodontal ligament stem cells (PDLSCs), apical papillary stem cells (SCAP), and alveolar bone marrow stem cells (ABMSCs); they are derived from various dental tissues, including immature wisdom teeth, exfoliated deciduous teeth, apical papilla, periodontal ligament, and dental follicle tissue (Huang *et al.*, 2009; Potdar and Jethmalani, 2015). The periodontal ligament (PDL) is a soft connective tissue located between the cementum and the alveolar bone, providing tooth nutrition to maintain homeostasis and regeneration of periodontal tissue. PDL contains different cell types as well as a group of stem cells (Alvarez *et al.*, 2015). The PDLSCs express the mesenchymal stem cell markers CD13, CD90, and CD146, as well as bone-associated markers such as alkaline phosphatase (ALP) and bone sialoprotein (BSP), and have the potential to differentiate into osteoblasts, osteoblast-like cells, and periodontal ligament fibroblasts. PDLSCs eventually form typical alveolar bone/periodontium-like structures under defined culture conditions and are

*Address correspondence to: Kangjuan Yang, yangkj@ybu.edu.cn; Ki-Taek Lim, ktlim@kangwon.ac.kr
#These authors contributed equally to this work
Received: 18 November 2019; Accepted: 28 April 2020

Doi: 10.32604/biocell.2020.09170

considered to be potential sources of MSCs (Park *et al*., 2011, 2013). Although several methods have been studied to transport PDLSCs into periodontal defects, including cell mass, micro-tissue, and cell sheet engineering *in vivo* (Park *et al*., 2011; Jin and Choung, 2016), few studies described the clinical application of PDLSCs as they are difficult to handle during surgery, and there are challenges in retaining the transferred PDLSCs at the surgical site.

Histone deacetylase (HDAC) inhibitors were reported to inhibit proliferation and promote the differentiation of cancer cells in tumors and hematological malignancies. The mechanism of HDAC inhibitors involves the regulation of gene expression by increasing the acetylation of histones and non-histones (Marks, 2007; Kouraklis and Theocharis, 2006; Lee *et al*., 2015). HDAC inhibitors interact with lysine residues of histone proteins (H2A, H2B, H3, and H4), resulting in the removal of acetyl moieties. Acetylation results in the formation of positive charges on lysine residues, which inactivate the function of the native protein. Thus, histone deacetylation is generally associated with the suppression of gene expression (Richon, 2006; Duncan *et al*., 2015). Moreover, it was reported that HDAC inhibitors could induce Runx2-dependent osteoblast differentiation by suppressing adipocyte differentiation *in vitro* (Fischer *et al*., 2010; Dudakovic *et al*., 2013).

Suberoylanilide hydroxamic acid (SAHA), a new class of broad-spectrum histone deacetylase inhibitor, was reported to enter phases I and II clinical trials for application in cancer treatment (Marks, 2007). SAHA resembles HDAC in structure and function; it inhibits cell cycle progression and induces apoptosis to disrupt gene function (Richon, 2006). Moreover, SAHA induces cardiomyogenic differentiation of human dental follicle-derived stem cells by regulating the cardiomyogenic transcription factors *TNNT2*, *α-SMA*, and *Desmin* (Sung *et al*., 2016). Previously, SAHA was reported to enhance bone resorption and reduce mineral density (Sato *et al*., 2001; Kwon *et al*., 2012). However, the role of SAHA in odontoblastic differentiation and corresponding signaling pathways have not been elucidated extensively. Thus, our present study investigated the effects of SAHA on osteoblast differentiation as well as the mineralization potential of hPDLSCs *in vitro*. Further, we demonstrated that SAHA induces osteoblast differentiation via ERK/MAPK signaling pathways.

Materials and Methods

Human PDLSC cultures

Human periodontal ligaments were extracted and obtained from the third molar tooth of adult humans. All the experiments regarding dental implantations, stem cell isolation, and maintenance were approved by the Department of Stomatology, Institutional Review Board, affiliated with the Hospital of Yanbian University (Yanbian, China; IRB number 2019201). Written consent letters were obtained from all the donors. Human periodontal ligaments were gently scraped with forceps from the third molar and digested for 1 h with 3 mg/mL collagenase type-1 (Worthington Biochem. Co., NJ, USA) and 4 mg/mL dispase (Boehringer, UK) at 37°C. After digestion, the remaining cells were cultured in an alpha modification of Eagle's medium (α-MEM; Gibco-BRL, USA) supplemented with 10% fetal bovine serum (FBS; Gibco-BRL, USA), 2 mM glutamine, 100 mM ascorbic acid-2-phosphate, and 1% antibiotics (Gibco-BRL; 100 U/mL penicillin and 100 mg/mL streptomycin) and incubated at 37 ± 1°C with 5% CO_2. The medium was replaced every 48 h. For our study, we selected hPDLSCs from three different donors. The second or third passage of cells was used for all the experiments.

Cytotoxicity evaluation

The cytotoxicity of hPDLSCs in the presence of SAHA was evaluated using a 3-(4,5-dimethylthiazol-2-yl)-2,5-diphenyltetrazolium bromide (MTT) assay kit per the manufacturer's instructions (Promega, Wisconsin, USA). Briefly, hPDLSCs (3×10^3 cells/well) were cultured in 96-well plates for 48 h. Varying amounts of SAHA were added to 100 µL of the culture medium per well to achieve final concentrations of 0, 100, 300, 500, 800, 1000, and 2000 ng/mL. After incubation, a 15 µL premixed dye solution was added and incubated at 37°C for 4 h followed by addition of 100 µL stop solution. Finally, the end product was analyzed by measuring the optical density (OD) at 595 nm (Infinite® M Nano 200 Pro; TECAN, Switzerland). All samples were run in triplicate (n = 3), and data are presented as mean ODs ± standard deviations. Statistical significance was considered at $^*p < 0.05$.

Flow cytometry

For flow cytometry, 1×10^6 were fixed with 3.7% paraformaldehyde (Sigma-Aldrich, USA) for 10 min and resuspended in 1X phosphate-buffered saline (PBS; Gibco-BRL) containing 1% bovine serum albumin (BSA; ICN Biomedical Corp., CA, USA) for 30 min to block nonspecific antibody-binding sites. Next, cells were incubated with specific primary antibodies (CD34, CD13, CD90, or CD146) for 1 h at 4°C, followed by incubation with fluorescent secondary antibodies for 1 h at room temperature. All the antibodies were purchased from BD Biosciences (San Jose, CA, USA). Finally, the percentages of CD13, CD90, CD146 positive, and CD34 negative cells were measured using a FACS Caliber flow cytometer (BD Immunocytometry Systems, SJ, USA). Results were analyzed using the Cell Quest Pro software (BD Systems, SJ, USA).

Osteogenic, chondrogenic, and adipogenic differentiation

PDLSCs (1×10^4/well) were cultured in 24-well plates containing DMEM medium supplemented with 10% fetal bovine serum (FBS; Gibco-BRL) and 1% antibiotics (Gibco-BRL). Next, the cells were transferred to osteogenic (50 mg/mL ascorbic acid, 10 mM β-glycerophosphate, and 100 nM dexamethasone), chondrogenic (1% chondrogenic basal medium, 1% chondrogenic supplement, and 5 µg/mL gentamicin reagent), or adipogenic (1% adipocyte basal medium, 1% adipocyte supplement, and 5 µg/mL gentamicin reagent) differentiation medium (StemPro, Gibco-BRL) and cultured for three weeks. Subsequently, the cells were stained with 2% Alizarin Red S (ARS; pH 4.2; Sigma-Aldrich, USA), 1% Alcian Blue (Sigma-Aldrich), and 0.3% Oil Red O dye (Sigma-Aldrich) for the detection of

mineralized nodules (calcium deposition), proteoglycans, and fat vacuoles as indicators of osteogenic, chondrogenic, and adipogenic differentiation, respectively. Stained cells were visualized under an inverted optical microscope (Olympus U-SPT; Olympus, Japan).

Alkaline phosphatase staining

For ALP activity, hPDLSCs were cultured (4×10^4 cells/well) in 24-well plates with αMEM supplemented with 50 μg/mL ascorbic acid, 10 mM β-glycerophosphate, and 100 nM dexamethasone (Sigma-Aldrich) for seven days with or without SAHA (300 ng/mL) treatment. Before staining, cells were fixed in 10% formalin (DUKSAN Chemicals Co., Gyeonggi-do, Republic of Korea), rinsed with 1X PBS twice, incubated with 0.1% TritonX-100 for 5 min, and finally stained using the Leukocyte Alkaline Phosphatase Kit (Sigma-Aldrich) according to the manufacturer's protocol. After seven days of incubation, cells were gently washed twice with ice-cold PBS and lysed with 0.01% sodium dodecyl sulfate for 30 min. The supernatant was collected, and an assay buffer containing 2 mM magnesium chloride ($MgCl_2$), 0.5 M adenosine monophosphate (AMP; pH 10.0), and 9 mM p-nitrophenyl phosphate (pNPP) was used to measure ALP activity. Absorbance was measured at 405 nm. All samples were run in triplicate (n = 3). Data are presented as mean ODs ± standard deviations, and statistical significance was considered at $^*p < 0.05$.

Alizarin Red-S staining

To evaluate the biomineralization potential of hPDLSCs, ARS staining was performed as described previously (Dutta *et al.*, 2019). Briefly, hPDLSCs (4×10^4 cells/well) were seeded in 24-well plates in α-MEM containing 10% FBS and 1% antibiotics at 37 ± 1°C until reaching 50–60% confluence. The hPDLSCs were cultured in differentiation media with 50 mg/mL ascorbic acid, 10 mM b-glycerophosphate, and 100 nM dexamethasone (Sigma-Aldrich) for two weeks. Subsequently, the plates were rinsed twice with 1X PBS (pH 7.4) and fixed with 4% paraformaldehyde (Sigma-Aldrich) for 20 min. After fixation, the cells were stained with 40 mM ARS (pH 4.2; Sigma-Aldrich) for 15 min at room temperature and rinsed with distilled water, and mineralized nodules were visualized using an inverted optical microscope (Olympus U-SPT; Olympus, Japan). To quantify the mineral deposition (calcium deposition), the plates were washed with 500 μL destaining solution containing 10% cetylpyridinium chloride and 10 mM sodium phosphate for 10 min at room temperature. The absorbance of the destained solution was measured at 562 nm. All samples were run in triplicate (n = 3). Data are presented as mean ODs ± standard deviations, and statistical significance was considered at $^*p < 0.05$.

Western blot analysis

hPDLSCs (1×10^6 cells/dish) were cultured, collected, and lysed in RIPA buffer containing 1 mM phenylmethylsulfonyl fluoride. The supernatant was collected, and protein concentration was measured using the BSA Protein Assay Kit (Bio-Rad Laboratories, USA). An equal volume of protein was separated by sodium dodecyl sulfate-polyacrylamide gel electrophoresis, and the gel was transferred to a polyvinylidene difluoride membrane (GE Healthcare, Chicago, USA). Primary antibodies against *Runx2*, *ERK1/2*, *p-ERK1/2*, *JNK*, *p-JNK*, *P38*, and *p-P38* were purchased from Abcam, UK. *OPN, OSX, OCN, BSP, COL1*, and *ALP* were used for mechanism studies. Blots were developed using horseradish peroxidase-conjugated secondary antibodies (Cell Signaling Technology, MA, USA) and visualized using a chemiluminescence kit (GE Healthcare, Chicago, USA).

RNA isolation and real-time polymerase chain reaction (RT-qPCR) analysis

To study the gene expression in the presence of SAHA, hPDLSCs (1×10^6 cells/well) were cultured for two weeks in osteogenic induction medium. The RNeasy Mini Kit (Qiagen, Germany) was used to extract total RNA from the samples. RNA and cDNA sample purities and concentrations were determined spectrophotometrically (Infinite® M Nano 200 Pro; TECAN). Approximately, 2 μg of RNA was used to synthesize cDNA. RNA expression was quantified using RT-qPCR with an ABI PRISM 7500 sequence detection system (Applied Biosystems, Carlsbad, CA, USA). The reaction conditions included 40 cycles of denaturation for 15 s at 95°C followed by amplification at 60°C. All reactions were run in triplicate (n = 3) and normalized to the housekeeping gene, glyceraldehyde-3-phosphate dehydrogenase (*GAPDH*). The relative mRNA expression levels of the control and SAHA-treated groups were calculated and compared using the ΔC_T method. For real-time PCR, the specific primers for *OPN*, *OCN*, *BSP*, *Col1*, *Runx2*, *ALP*, and *GAPDH*, were synthesized as listed in Tab. 1.

Statistical analysis

Statistical analysis was carried out by one-way ANOVA using Statistical Package for Social Science 22.0 software (SPSS 22.0, Inc., USA). All data shown are mean ± SD of triplicate (n = 3) experiments, and statistical significance was considered as $^*p < 0.05$.

Results

Characterization of hPDLSCs cells

Human PDLSCs were isolated from the third molar tooth of humans and cultured in α-MEM medium. After seven days of primary culture, fibroblast-like colonies were observed (Fig. 1A). Passage three (P_3) cells were used for the characterization study. Next, to investigate the immunophenotypic markers associated with hPDLSCs, we performed flow cytometry. FACS analysis showed that approximately 99.93% of hPDLSCs expressed CD13, 99.85% expressed CD90, 84.13% expressed CD146, and 10.71% expressed CD34 markers (Fig. 1B). The relative intensity of antibody binding to cells was quantified to determine the percentage of positive cells. CD34, preliminary recognized as a negative marker, represented primitive hematopoietic progenitors and endothelial cells. In contrast, CD13, CD90, and CD146 were putative positive markers of MSCs. These results indicate that hPDLSCs displayed morphological as well as phenotypic characteristics of MSCs.

TABLE 1

Prime sequences used for real-time polymerase chain reaction (RT-qPCR)

No.	Genes	*Genbank* No.	Sequences (5'-3')	References
1	*OPN*	J04765	CCCACAGACCCTTCCAAGTA ACACTATCACCTCGGCCATC	Young *et al.*, 1990
2	*OCN*	X53698	GTGCAGAGTCCAGCAAAGGT TCAGCCAACTCGTCACAGTC	Kiefer *et al.*, 1990
3	*Col1*	XM_012651	CTGACCTTCCTGCGCCTGATGTCC GTCTGGGGCACCAACGTCCAAGGG	NCBI Annotation Project, 2002
4	*ALP*	BC090861	GGACATGCAGTACGAGCTGA GCAGTGAAGGGCTTCTTGTC	Strausberg *et al.*, 2002
5	*BSP*	NM_004967	CAACAGCACAGAGGVAGAAA CGTACTCCCCCTCGTATTCA	Oldberg *et al.*, 1988
6	*Runx2*	NM_001015051	CGCATTCCTCATCCCAGTAT GACTGGCGGGGTGTAAGTAA	Xu *et al.*, 2019
7	*GAPDH*	NM_005253678	ACCACAGTCCATGCCATCAC TCCACCACCCTGTTGCTGTA	Mondragón *et al.*, 2019

Abbreviations: *OPN*, osteopontin; *OCN*, osteocalcin; *Col1*, type 1 collagen; *ALP*, alkaline phosphatase; *BSP*, bone sialoprotein; *Runx2*, runt-related transcription factor 2; *GAPDH*, glyceraldehyde-3-phosphate dehydrogenase.

Tri-lineage differentiation potential of hPDLSCs

To observe the multilineage differentiation potential of hPDLSCs at P_3, the cells were allowed to differentiate in osteogenic, chondrogenic, or adipogenic medium *in vitro*. After three weeks of osteogenic induction, hPDLSCs successfully differentiated into osteocytes. ARS staining showed an intense color due to the mineral deposition throughout the adhesion layer (Fig. 2A). Furthermore, the cells were also able to undergo adipogenic and chondrogenic differentiation after treatment with specific adipogenic and chondrogenic supplements. Alcian Blue and oil Red-O staining showed the synthesis of proteoglycans (Fig. 2B) and lipid droplets (Fig. 2C), respectively.

SAHA treatment promotes hPDLSCs proliferation

It was reported earlier that SAHA induced the proliferation of dental pulp stem cells (DPSCs) without altering their morphology (Duncan *et al.*, 2012). The effect of SAHA on *in vitro* proliferation of hPDLSCs was evaluated by MTT assay, as indicated in Fig. 3. Human PDLSCs were seeded in 96-well plates and treated with different concentrations of SAHA (0, 100, 300, 500, 800, 1000, and 2000 ng/mL). After 24 h incubation, cell proliferation was not inhibited with increasing concentrations of SAHA (Fig. 3A). Notably, 2000 ng/mL SAHA still had no cytotoxicity to hPDLSCs as compared to the control samples after 48 h of incubation, as indicated in Fig. 3B. In particular, there was a significant increase in cell viability at 300 ng/mL concentration ($^*p < 0.05$) as compared to the control samples ($^*p < 0.05$) after 24 and 48 h. Thus, our results suggested that 300 ng/mL is the optimum SAHA concentration for hPDLSCs proliferation.

SAHA-induced in vitro differentiation of hPDLSCs

To investigate the effects of SAHA on osteoblast differentiation *in vitro*, we performed Alizarin Red-S (ARS) and alkaline phosphatase (ALP) staining. The hPDLSCs were cultured in osteogenic differentiation medium and treated with or without SAHA (0 or 300 ng/mL) for two weeks. After two weeks, the plates were washed and stained with 40 mM ARS and ALP staining kit to evaluate mineralization efficiency. Interestingly, the SAHA-treated cells showed more intense color after ALP (Fig. 4A) and ARS (Fig. 4B) staining compared to control samples. The ALP activity was significantly increased in SAHA-treated (300 ng/mL) cells compared to control. Furthermore, ARS staining showed a significant increase in calcium content in the presence of 300 ng/mL SAHA, as shown in Fig. 4C.

Osteoblast-specific genes and proteins expression

To evaluate the gene and protein expression related to osteoblast differentiation, we conducted real-time PCR and western blotting. The expression levels of relative markers, including osteopontin (*OPN*), osteocalcin (*OCN*), collagen type-1 (*COL1*), alkaline phosphatase (*ALP*), bone sialoprotein (*BSP*), and runt-related transcription factor (*RUNX2*) were significantly increased after treatment with 300 ng/mL SAHA as shown in Fig. 5A. To explore the protein expression of SAHA-treated hPDLSCs, we evaluated expression levels by western blotting. We found that the expression of transcription factors, such as glioma-associated protein (GLI1), runt-related transcription factor-2 (RUNX2), and osterix (OSX), were significantly elevated by SAHA treatment as compared to the control group (Fig. 5B). GLI1 was known previously to induce early osteoblast differentiation in a RUNX2-dependent and independent manner in early osteoblast differentiation (Hojo *et al.*, 2012).

SAHA induces osteoblast differentiation via ERK/MAPK signaling pathway

To investigate the signaling mechanism related to osteoblast differentiation, we also evaluated the expression of ERK/MAPK signaling pathway-associated proteins, such as extracellular receptor kinase (ERK), phosphorylated ERK (p-ERK), mitogen-activated protein kinases (p-38 and p-p38),

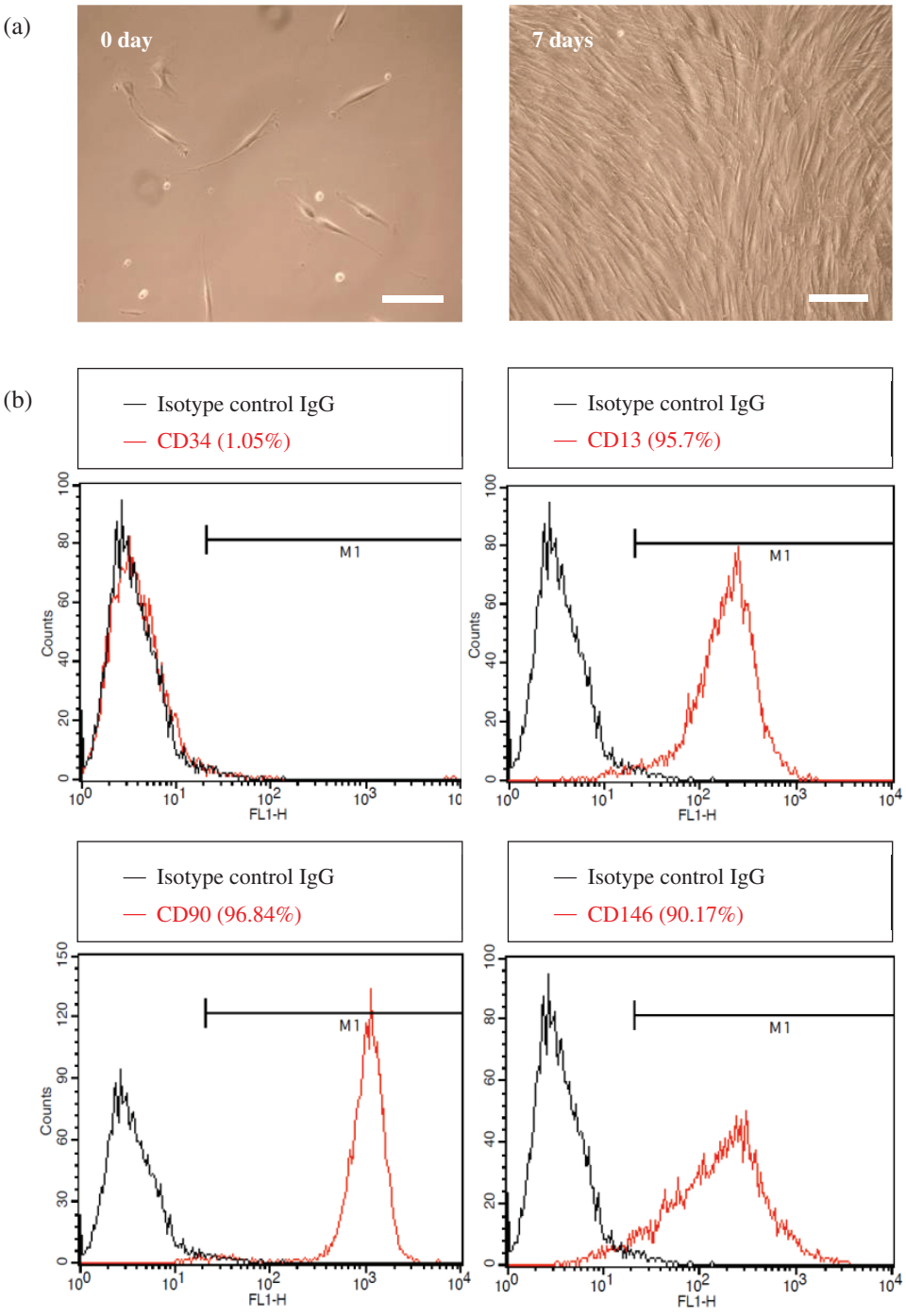

FIGURE 1. Characterization of human periodontal ligament stem cells (hPDLSCs).
(A) Photomicrograph of the cultured hPDLSCs at passage three (P_3) showing fibroblast-like morphology after 7 days of primary culture (Magnification, 10×). **(B)** Fluorescence-activated cell sorting (FACS) analysis of hPDLSCs with mesenchymal stem cell markers, including CD13, CD34, CD90, and CD146. The populations of $CD13^+$, $CD34^-$, $CD90^+$, and $CD146^+$ cells were analyzed, and the percentage of cells to the right side of the M1 gate was measured (n = 3).

and c-Jun-N-terminal kinases (JNK and p-JNK). The relative expression of ERK was upregulated after treatment with 300 ng/mL SAHA. While a significant increase ($^*p < 0.05$) of ERK was observed in the SAHA-treated group (Fig. 6), there was no significant increase in the expression of MAPK signaling pathway-associated protein, p-p38, as compared to the control samples. Our findings further demonstrate that SAHA enhances the osteogenic differentiation by the MAPK/ERK signaling pathway and that RUNX2, which is downstream of MAPK signaling, plays a crucial role in this process.

Discussion

HDAC inhibitors are promising drugs for the treatment of cancer as they have been shown to have antitumor activities, such as the ability to inhibit cell proliferation (Martinez-Iglesias *et al.*, 2008). SAHA, a new class of HDAC inhibitors, has been identified recently as an effective anti-cancer drug. SAHA enhances gene expression by increasing the acetylation of histones and non-histone proteins. It was also reported that SAHA could modulate differentiation (Jeon *et al.*, 2006). Kwon *et al.* (2012) reported that SAHA (5 μM) induced the differentiation potential of mouse dental papilla cells (MDPC23) *in vitro*. Moreover, they showed that SAHA increased the expression of DSPP during odontoblast differentiation. SAHA-induced growth, viability, apoptosis, and mineralization of dental pulp cells (DPCs) has also been reported (Duncan *et al.*, 2015; Wang *et al.*, 2014), which led us to hypothesize that SAHA induces the differentiation of

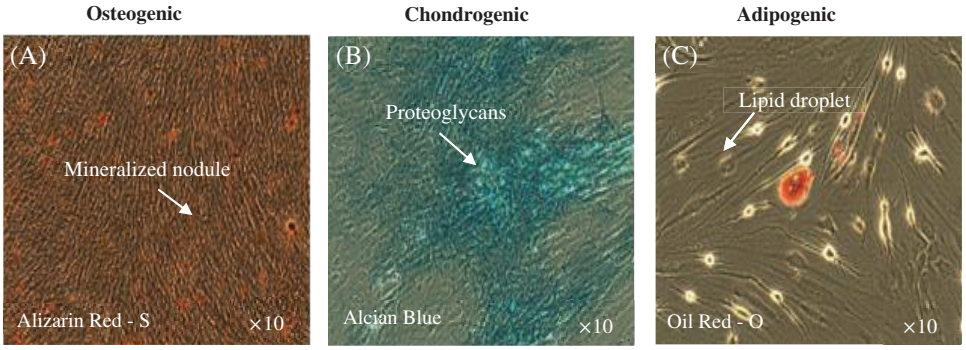

FIGURE 2. The tri-lineage differentiation potential of hPDLSCs. The cells were cultured in osteogenic, chondrogenic, and adipogenic medium for three weeks, respectively. Alizarin Red-S **(A)**, Alcian blue **(B)**, and Oil Red-O **(C)** staining showed the progress of differentiation (Magnification, 10×).

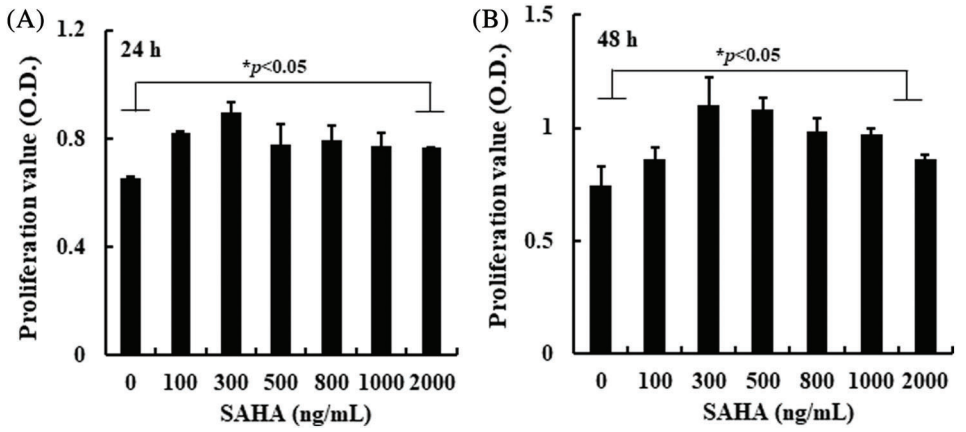

FIGURE 3. Cytotoxicity evaluation of hPDLSCs in the presence of SAHA at indicated time intervals.
To investigate the effect of SAHA on hPDLSCs cell proliferation *in vitro*. The cells were treated with SAHA for 24 h **(A)** and 48 h **(B)**. The proliferation value was represented as mean optical density (mean O.D.) of 595 nm. All data shown are mean ± SD of triplicate experiments (n = 3), statistical significance was considered as $^*p < 0.05$.

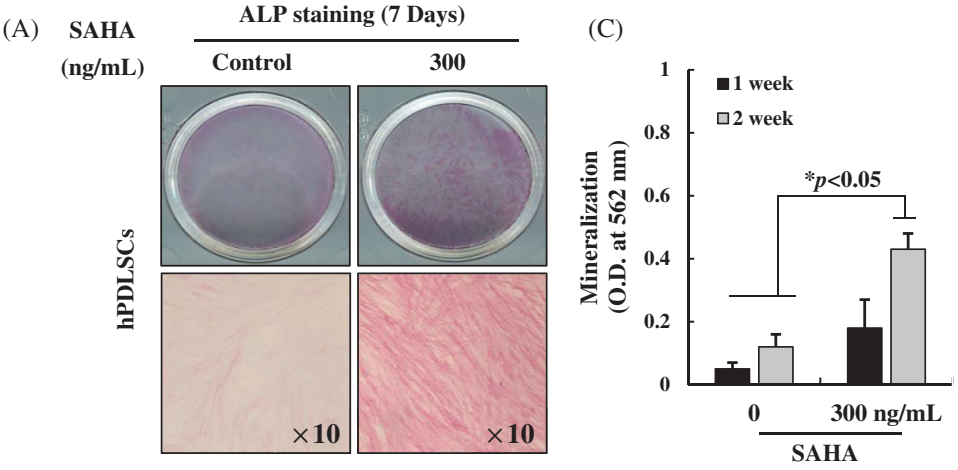

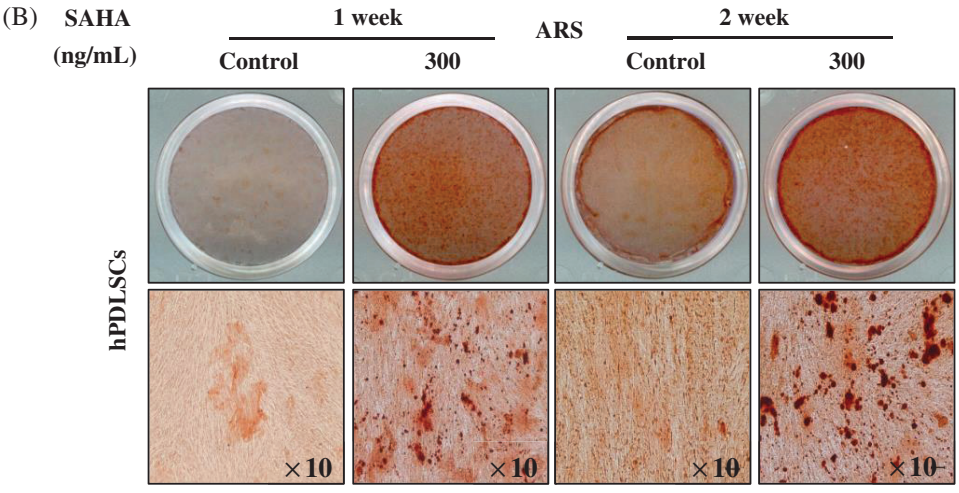

FIGURE 4. The mineralization efficiency of hPDLSCs in the presence of SAHA; the hPDLSCs were cultured in osteogenic differentiation medium without or with SAHA (0 and 300 ng/mL).
(A) ALP staining After 5 days of incubation (Magnification, 10×). **(B)** Alizarin Red-S staining and mineralization was performed after 1 and 2 weeks of incubation (Magnification ×10). All data shown are mean ± SD of triplicate experiments (n = 3). Statistical significance was considered as $^*p < 0.05$.

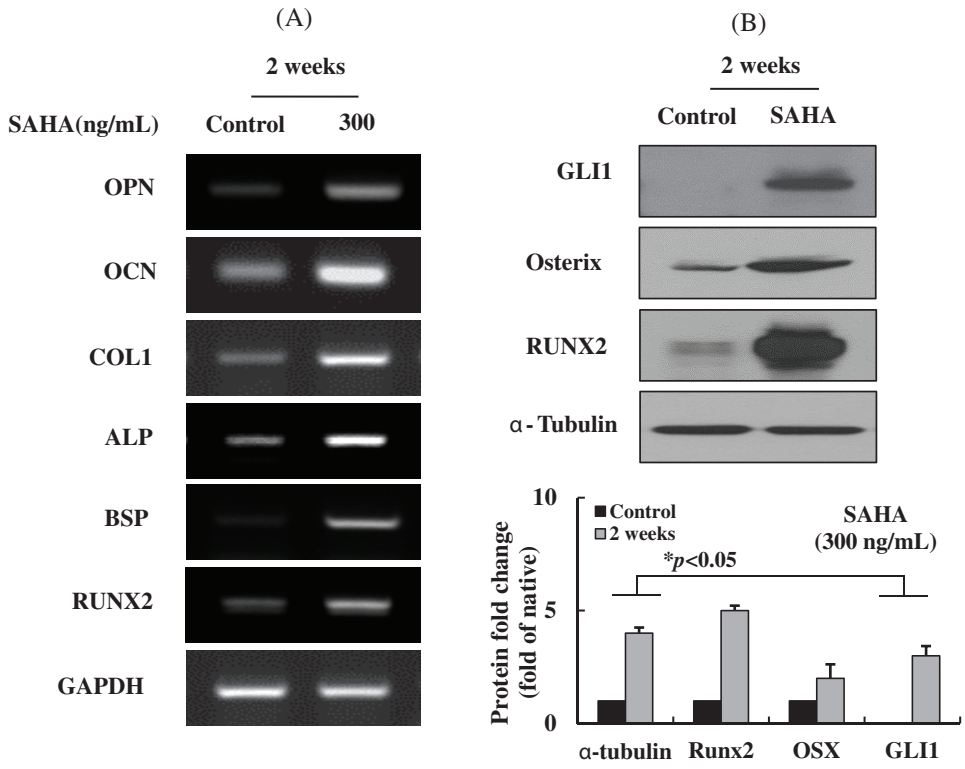

FIGURE 5. SAHA-induced osteogenesis in hPDLSCs. **(A)** Real-time PCR (qPCR) analysis of the osteoblast-specific gene markers (*Runx2, BSP, ALP, COL1, OCN*, and *OPN*). hPDLSCs without SAHA-treatment were considered as control. The relative mRNA expression was evaluated and normalized to the housekeeping gene (*GAPDH*). **(B)** Western blot analysis for the expression of Runx2, OSX, and GLI1 after 2 weeks of post-treatment by SAHA. Blots were quantified by ImageJ software and the quantification graph showing the relative change in protein expression, respectively. Data from at least three (n = 3) independent measurements, statistical significance was considered as $^{*}p < 0.05$.

human periodontal ligament stem cells (hPDLSCs) *in vitro*. Consistent with our hypothesis, we demonstrated that SAHA stimulates the osteogenic differentiation of hPDLSCs by inducing their proliferation.

SAHA can promote the differentiation of hPDLSCs into osteoblasts and result in the formation of alveolar bone. Recently, "The Mesenchymal and Tissue Stem Cell Committee of the International Society for Cellular Therapy," proposed a criterion to define MSCs. MSCs must express markers such as CD10, CD13, CD29, CD44, CD59, CD90, CD105 and CD146, and lack expression of the markers, CD14, CD34, CD45, HLA-DR (Lei *et al.*, 2014). Human PDLSCs isolated from the periodontal ligament of the third molars also exhibit fibroblast-like appearance upon confluence. Dental stem cells have also been shown to express some stemness markers, such as Nanog, Oct4, and Sox2 by RT-qPCR. Our results suggest that hPDLSCs isolated from molar teeth are characteristic of hMSCs as they highly express positive markers such as CD13, CD90, and CD146 and do not express negative markers, such as CD34.

CD146 was initially recognized as an adhesion molecule in melanoma cells but is currently used as a marker for the identification for endothelial cell lineages (Sung *et al.*, 2016). Notably, the presence of CD146 positive hPDLSCs showed significant proliferative and osteogenic potential (Zhu *et al.*, 2013). Thus, MSCs must be able to differentiate into osteoblasts, adipocytes, and chondroblasts *in vitro*. Previously, it was reported that human PDLSCs contain a population of postnatal multipotent stem cells that can be isolated using explant cultures or enzymatic digestion and expanded *in vitro* (Choi *et al.*, 2015; Kim *et al.*, 2015; Osathanon *et al.*, 2013; Saghiri *et al.*, 2018; Seo *et al.*, 2004; Lee *et al.*, 2014; Zhao and Liu, 2014). Our results show that hPDLSCs differentiate successfully into osteocytes, chondrocytes, and adipocytes after *in vitro* culture in supplemented medium, as reported previously (Sung *et al.*, 2016). These results indicate that hPDLSCs are the richest sources of stem cells for osteoinduction, and SAHA could enhance the differentiation potential of hPDLSCs. Further, our investigation showed that SAHA can increase ALP activity and calcium deposition in hPDLSCs, as noted in previous reports (Kwon *et al.*, 2012). These results further elucidated the effect of SAHA on the differentiation of hPDLSCs.

In this study, SAHA showed significant effects on enhancing matrix mineralization and osteoblast-specific gene marker expression in hPDLSCs. Initially, SAHA was chosen for *in vitro* differentiation of hPDLSCs because it is clinically relevant and exhibits a stronger osteoinduction potential than other HDAC inhibitors. Osteogenic and odontogenic differentiation is related to a variety of bone-related markers, such as Runx2, Osterix, ALP, OCN, BSP, OPN, and Col1 (Fu *et al.*, 2014; Ge *et al.*, 2018; d'Alessandro *et al.*, 2013; Jin *et al.*, 2015). Previously, it was reported that HDAC inhibitors like SAHA stimulate osteoblast differentiation by increasing the acetylation of Runx2, a transcription factor critical for osteoblast differentiation and migration (Schroeder *et al.*, 2004). Acetylation of Runx2 increases protein stability and up-regulates the expression of another transcription factor, Dspp. However, in mature odontoblasts, Runx2 was found to downregulate the expression of Dspp (Kwon *et al.*, 2012). Notably, mutations in the Runx2 gene were found to inhibit the terminal differentiation of odontoblasts, indicating the role of Runx2 in osteoblast differentiation (Miyazaki *et al.*, 2008). Kwon *et al.* (2012) reported that a 5 μM concentration of SAHA was sufficient to modulate the

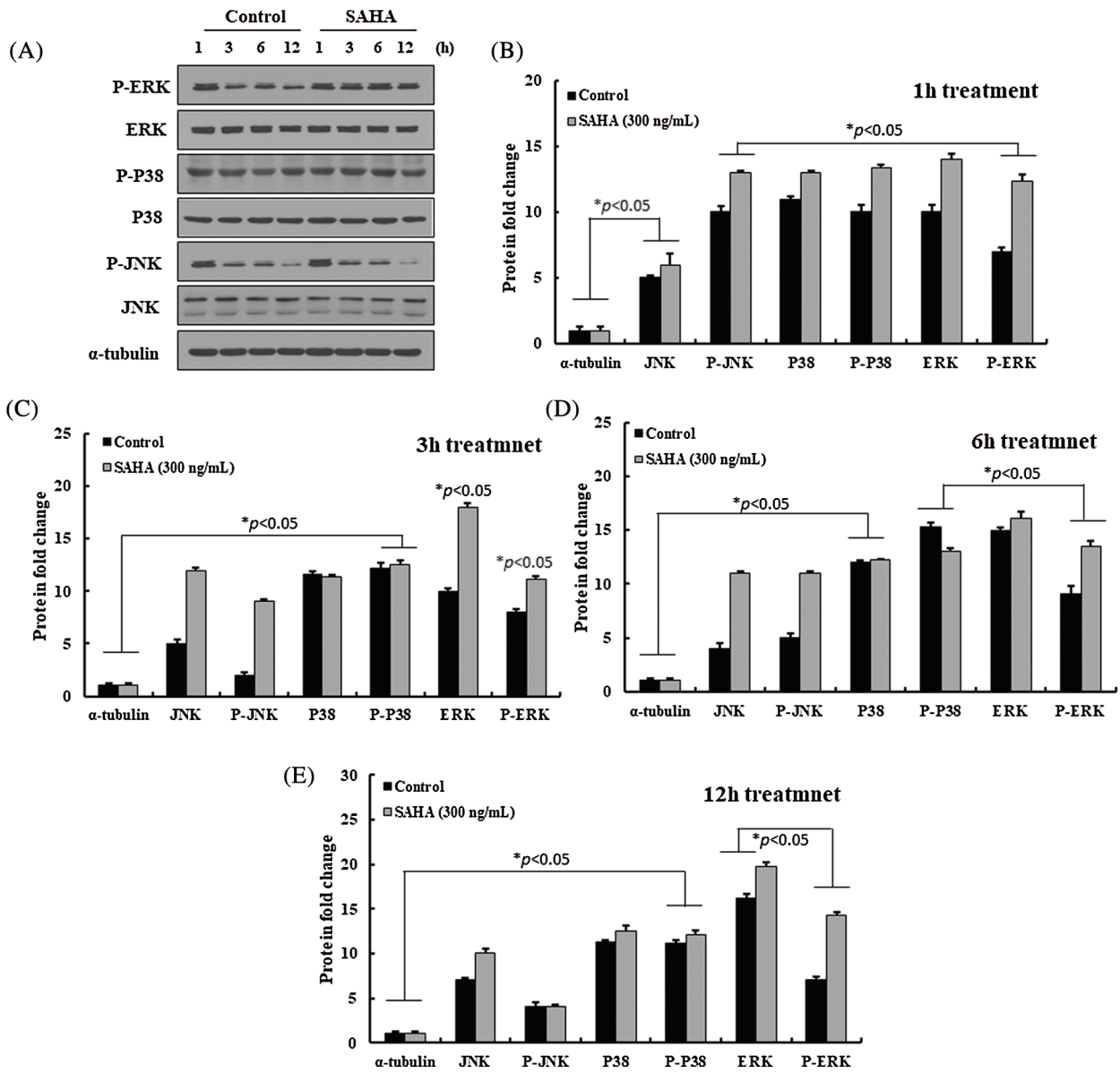

FIGURE 6. (A) Screening for the ERK/MAPK signaling associated proteins (JNK, p-JNK, p38, p-P38, ERK, and p-ERK) by western blot analysis. **(B)** Blots were quantified by ImageJ software and data was normalized to control (α-tubulin). All data shown are mean ± SD of triplicate experiments (n = 3). Statistical significance was considered as $^*p < 0.05$.

expression of Runx2. They also showed that SAHA promotes the acetylation of histone H3. Another study reported that HDAC-8 regulates osteogenesis of hMSCs by regulating the level of H3K9Ac and Runx2 acetylation (Fu *et al.*, 2014). In consideration of these previous studies, we investigated the effects of SAHA (300 ng/mL) on relative mRNA expression of OPN, OCN, Col1, BSP, ALP, and Runx2 in hPDLSCs. Notably, an increase in Runx2, OCN, BSP, OPN, and Col1 mRNA expression was noticed, further indicating that 300 ng/mL of SAHA is effective for osteoblast-specific gene marker expression. Similarly, it was reported that Valproic acid (VPA) and Trichostatin A (TSA) enhanced the expression of OCN and BSP in human DPSCs (Paino *et al.*, 2013; Duncan *et al.*, 2013). Furthermore, our results indicate that SAHA also upregulated the level GLI1, OSX, and Runx2 proteins. These data suggest that SAHA might regulate Runx2 and OSX expression during the differentiation of hPDLSCs. Runx2, core-binding factor 1 (CBFA1)/osteogenic specific factor 2 (OSF2), is a member of the Runt domain transcription factor family and is critical for embryo development. Runx2 binds to specific promoters and regulates the transcription of several genes (e.g., Oct4, Nanog) that play a crucial role in osteoclast formation, chondrocyte development, bone matrix formation, and subsequent bone mineralization (Lee *et al.*, 2011b; Hu *et al.*, 2015; Xia *et al.*, 2011). Osterix is a zinc finger-containing transcription factor encoded by the Sp7 gene that regulates gene expression in committed osteoblast precursor cells. Osterix is also a transcription factor essential for osteoblast differentiation, acting downstream of Runx2 (Shi *et al.*, 2016). In addition to OSX, GLI1 is thought to play a crucial role in mediating transcriptional responses in early osteoblast differentiation (Hojo *et al.*, 2012). During osteogenic differentiation, both Runx2 and Osterix, along with GLI1 regulate the expression of

significant bone marker genes, including OPN, OCN, and type I collagen expressed by chondrocytes and osteoblasts.

In our present study, SAHA showed a significant increase in ERK/MAPK signaling-related protein expression that is critical for osteoblast-osteoclast development. Previous reports have shown that the mitogen-activated protein kinase (MAPK) signaling pathway plays an essential role in the regulation of osteogenic differentiation of BMSCs (Lee *et al.*, 2011a; Ren *et al.*, 2015; Xia *et al.*, 2011; Iwasaki *et al.*, 2013; He *et al.*, 2016; Li *et al.*, 2013; Yu *et al.*, 2012; Jun *et al.*, 2010). The MAPK family proteins, such as extracellular signal-regulated kinase (ERK), c-Jun N-terminal kinase (JNK), and p38 MAPK (p38), have been reported to induce osteogenic differentiation (He *et al.*, 2016; Yu *et al.*, 2012). In particular, ERK1/2 is activated continuously during cell transformation, proliferation, and survival. Also, p38 is involved in a variety of cellular responses including cell cycle control, inflammatory responses, apoptosis, and the differentiation of several cell types, including osteoblasts (Ren *et al.*, 2015; Li *et al.*, 2013).

Interestingly, previous findings suggested that Runx2 is a downstream regulator of the ERK1/2 pathway. Phosphorylation of ERK1/2 induces the expression of Runx2 during osteoblast differentiation and skeletal development (Yin *et al.*, 2015; Jeon *et al.*, 2006; Schroeder *et al.*, 2004; Feng *et al.*, 2009). In conjunction with that research, our study revealed that the phosphorylation levels of ERK and the activation of Runx2 were upregulated in the SAHA treated groups. However, the expression of p-JNK and p-p38 did not increase in our study. Collectively, our data strongly suggests that SAHA promotes the phosphorylation of ERK1/2, which in turn upregulated the transcriptional activity of Runx2, leading to the osteogenesis in hPDLSCs.

Our study was limited in that we used the periodontal ligament stem cells instead of other dental cells, such as dental pulp stem cells or apical papillary cells. Although we have investigated the role of SAHA on hPDLSC differentiation, it is also critical to investigate the effects of SAHA on chondrogenesis, neurogenesis, and adipogenesis. Data from this study demonstrates that SAHA enhances hPDLSC differentiation by regulating the expression of Runx2, OSX, and other transcription factors via the ERK/MAPK signaling pathway. However, to investigate the therapeutic potential of SAHA, further studies on other types of dental cells are required.

Conclusions

This study investigated the role of SAHA on the *in vitro* differentiation of human periodontal ligament stem cells (hPDLSCs). We investigated the cytotoxicity, *in vitro* differentiation (Alizarin Red-S and alkaline phosphatase), RT-qPCR, and western blotting as direct indicators of osteogenesis. Here we present an outline of SAHA-induced hPDLSC differentiation based on preliminary findings. The cell viability of SAHA-treated cells (300 nM) was increased by 20% ($^*p < 0.05$) as compared to the control groups ($^*p < 0.05$) after 48 h incubation. As a result, both cell viability and proliferation were increased significantly at 24 and 48 h. Gene expression is directly related to functional protein synthesis.

Osteoblast-specific gene expression studies revealed that the expression of *Runx2*, *ALP*, *OCN*, and *COL1* was significantly increased ($^*p < 0.05$) in the SAHA-treated cells after two weeks in culture. These results were also validated by Western blot analysis. The MAPK/ERK1/2 family protein expression was also studied to understand the role of MAPK signaling during osteoblast differentiation. Interestingly, ERK and p-JNK expression were significantly increased by 12.8% ($^*p < 0.05$) and 8.7% ($^*p < 0.05$), followed by a 24% increase in Runx2 expression ($^*p < 0.05$), respectively. These results suggest that ERK might be a positive regulator of Runx2 transcription factors. In conclusion, the present findings suggest that SAHA treatment (300 ng/mL) can stimulate osteoblast maturation by the MAPK/ERK1/2 signaling pathway.

Author Contributions: X. Y. Z., S. D. D., J. B., and L. M. M. contributed to the data acquisition, analysis, and writing of the manuscript; J. B., X. Y. Z, and J. Z. H. designed the study, and S. D. D. revised the manuscript. All the authors gave final approval and agreed to be accountable for all aspects of the work.

Funding Statement: This research was supported by the Basic Science Research Program through the National Research Foundation of Korea (NRF) and funded by the Ministry of Education (No. 2018R1A6A1A03025582) and the National Research Foundation of Korea (NRF- 2019R1D1A3A03103828). The authors are also thankful to the Yanbian University Youth Project of China (No. 201804).

Conflicts of Interest: The authors declare that they have no conflicts of interest to report regarding the present study.

References

Alvarez R, Lee HL, Wang CY, Hong C (2015). Characterization of the osteogenic potential of mesenchymal stem cells from human periodontal ligament based on cell surface markers. *International Journal of Oral Science* **7**: 213–219. DOI 10.1038/ijos.2015.42.

Choi JK, Hwang HI, Jang YJ (2015). The efficiency of the *in vitro* osteo/dentinogenic differentiation of human dental pulp cells, periodontal ligament cells and gingival fibroblasts. *International Journal of Molecular Medicine* **35**: 161–168. DOI 10.3892/ijmm.2014.1986.

d'Alessandro L, Petrini M, Ferrante M, Di Marco S, Trubiani O, Spoto G (2013). Cyclic nucleotide phosphodiesterase activity in stem cells of human periodontal ligament (PDL-MSCs) before and after osteogenic induction. *Oral Surgery, Oral Medicine, Oral Pathology and Oral Radiology* **116**: e317–e323. DOI 10.1016/j.oooo.2012.02.023.

Dudakovic A, Evans JM, Li Y, Middha S, McGee-Lawrence ME, Wijnen AJV, Westerndorf JJ (2013). Histone deacetylase inhibition promotes osteoblast maturation by altering the histone H4 epigenome and reduces Akt phosphorylation. *Journal of Biological Chemistry* **288**: 28783–28791. DOI 10.1074/jbc.M113.489732.

Duncan HF, Smith AJ, Fleming GJ, Cooper PR (2012). Epigenetic modulation of dental pulp stem cells: implications for

regenerative endodontics. *International Endodontic Journal* **49**: 431–446.

Duncan HF, Smith AJ, Fleming GJP, Partridge NC, Shimizu E, Moran GP, Cooper PR (2015). The histone-deacetylase-inhibitor suberoylanilide hydroxamic acid promotes dental pulp repair mechanisms through modulation of matrix metalloprotenase-13 activity. *Journal of Cellular Physiology* **2015**: 798–816.

Duncan HF, Smith AJ, Fleming GP, Cooper PR (2013). Histone deacetylase inhibitors epigenetically promote reparative events in primary dental pulp cells. *Experimental Cell Research* **10**: 1534–1543. DOI 10.1016/j.yexcr.2013.02.022.

Dutta SD, Patel DK, Seo YR, Park CW, Lee SH, Kim JW, Kim J, Seonwoo H, Lim KT (2019). *In vitro* biocompatibility of electrospun poly (e-caprolactone)/cellulose nanocrystals nanofibers for tissue engineering. *Journal of Nanomaterials* **2019**: 1–11. DOI 10.1155/2019/2061545.

Feng C, Zhu J, Zhao L, Lu T, Zhang W, Liu Z, Tian J (2009). Suberoylanilide hydroxamic acid promotes cardiomyocyte differentiation of rat mesenchymal stem cells. *Experimental Cell Research* **315**: 3044–3051. DOI 10.1016/j.yexcr.2009.05.005.

Fischer A, Sananbenesi F, Mungenast A, Tsai LH (2010). Targeting the correct HDAC(s) to treat cognitive disorders. *Trends in Pharmacological Sciences* **31**: 605–617. DOI 10.1016/j.tips.2010.09.003.

Fu Y, Zhang P, Ge J, Cheng J, Dong W, Yuan H, Du Y, Yang M, Sun R, Jiang H (2014). Histone deacetylase 8 suppresses osteogenic differentiation of bone marrow stromal cells by inhibiting histone H3K9 acetylation and RUNX2 activity. *International Journal of Biochemistry & Cell Biology* **54**: 68–77. DOI 10.1016/j.biocel.2014.07.003.

Ge Y, Li J, Hao Y, Hu Y, Chen D, Wu B, Fang F (2018). MicroRNA-543 functions as an osteogenesis promoter in human periodontal ligament-derived stem cells by inhibiting transducer of ERBB2, 2. *Journal of Periodontal Research* **53**: 832–841. DOI 10.1111/jre.12572.

He Y, Jian CX, Zhang HY, Zhou Y, Wu X, Zhang G, Tan YH (2016). Hypoxia enhances periodontal ligament stem cell proliferation via the MAPK signaling pathway. *Genetics and Molecular Research* **15**: 1–10.

Hojo H, Ohba S, Yano F, Saito T, Ikeda T, Nakajima K, Komiyama Y, Nakagata N, Suzuki K, Takato T, Kawaguchi H, Chung U (2012). Gli1 protein participates in Hedgehog-mediated specification of osteoblast lineage during endochondral ossification. *Journal of Biological Chemistry* **287**: 17860–17869. DOI 10.1074/jbc.M112.347716.

Hu N, Feng C, Jiang Y, Miao Q, Liu H (2015). Regulative effect of Mir-205 on osteogenic differentiation of bone mesenchymal stem cells (BMSCs): possible role of SATB2/Runx2 and ERK/MAPK pathway. *International Journal of Molecular Sciences* **16**: 10491–10506. DOI 10.3390/ijms160510491.

Huang GJ, Gronthos S, Shi S (2009). Mesenchymal stem cells derived from dental tissues *vs.* those from other sources: their biology and role in regenerative medicine. *Journal of Dental Research* **88**: 792–806. DOI 10.1177/0022034509340867.

Iwasaki K, Komaki M, Yokoyama N, Tanaka Y, Taki A, Honda I, Kimura Y, Takeda M, Akazawa K, Oda S, Izumi Y (2013). Periodontal regeneration using periodontal ligament stem cell-transferred amnion. *Tissue Engineering Part A* **20**: 693–704.

Jeon EJ, Lee KY, Choi NS, Lee MH, Kim HN, Jin YH, Ryoo HM, Choi JY, Yoshida M, Nishino N, Oh BC, Lee KS, Lee YH, Bae SC (2006). Bone morphogenetic protein-2 stimulates Runx2 acetylation. *Journal of Biological Chemistry* **281**: 16502–16511. DOI 10.1074/jbc.M512494200.

Jin B, Choung PH (2016). Recombinant human plasminogen activator inhibitor-1 accelerates odontoblastic differentiation of human stem cells from apical papilla. *Tissue Engineering Part A* **22**: 721–732. DOI 10.1089/ten.tea.2015.0273.

Jin H, Choung HW, Lim KT, Jin B, Jin C, Chung JH, Choung PH (2015). Recombinant human plasminogen activator inhibitor-1 promotes cementogenic differentiation of human periodontal ligament stem cells. *Tissue Engineering Part A* **21**: 2817–2828. DOI 10.1089/ten.tea.2014.0399.

Jun JH, Yoon WJ, Seo SB, Woo KM, Kim GS, Ryoo HM, Baek JH (2010). BMP2-activated Erk/MAP kinase stabilizes Runx2 by increasing p300 levels and histone acetyltransferase activity. *Journal of Biological Chemistry* **285**: 36410–36419. DOI 10.1074/jbc.M110.142307.

Kim SY, An SY, Lee JS, Heo JS (2015). *Zanthoxylum schinifolium* enhances the osteogenic potential of periodontal ligament stem cells. *In Vitro Cellular & Developmental Biology-Animal* **51**: 165–173.

Kiefer MC, Saphire AC, Bauer DM, Barr PJ (1990). The cDNA and derived amino acid sequences of human and bovine bone Gla protein. *Nucleic Acids Research* **18**: 1909.

Kouraklis G, Theocharis S (2006). Histone deacetylase inhibitors: a novel target of anticancer therapy. *Oncology Reports* **15**: 489–494.

Kwon A, Park HJ, Baek K, Lee HL, Park JC, Woo KM, Ryoo HM, Baek JH (2012). Suberoylanilide hydroxamic acid enhances odontoblast differentiation. *Journal of Dental Research* **91**: 506–512. DOI 10.1177/0022034512443367.

Larsson L, Castilho RM, Giannobile WV (2015). Epigenetics and its role in periodontal diseases: a state-of-the-art review. *Journal of Periodontology* **86**: 556–568. DOI 10.1902/jop.2014.140559.

Lee CH, Huang YL, Liao JF, Chiou WF (2011a). Ugonin K promotes osteoblastic differentiation and mineralization by activation of p38 MAPK- and ERK-mediated expression of Runx2 and osterix. *European Journal of Pharmacology* **668**: 383–389. DOI 10.1016/j.ejphar.2011.06.059.

Lee JH, Lee DS, Choung HW, Shon WJ, Seo BM, Lee EH, Cho JY, Park JC (2011b). Odontogenic differentiation of human dental pulp stem cells induced by preameloblast-derived factors. *Biomaterials* **32**: 9696–9706. DOI 10.1016/j.biomaterials.2011.09.007.

Lee JS, Yi JK, An SY, Heo JS (2014). Increased osteogenic differentiation of periodontal ligament stem cells on polydopamine film occurs via activation of integrin and PI3K signaling pathways. *Cellular Physiology and Biochemistry* **34**: 1824–1834. DOI 10.1159/000366381.

Lee ZH, Kim HJ, Ryoo HM (2015). A novel osteogenic activity of suberoylanilide hydroxamic acid is synergized by BMP-2. *Journal of Bone Metabolism* **22**: 51–56. DOI 10.11005/jbm.2015.22.2.51.

Lei M, Li K, Li B, Gao LN, Chen FM, Jin Y (2014). Mesenchymal stem cell characteristics of dental pulp and periodontal ligament stem cells after *in vivo* transplantation. *Biomaterials* **35**: 6332–6343. DOI 10.1016/j.biomaterials.2014.04.071.

Li L, Han M, Li S, Wang L, Xu Y (2013). Cyclic tensile stress during physiological occlusal force enhances osteogenic differentiation of human periodontal ligament cells via ERK1/2-Elk1 MAPK pathway. *DNA and Cell Biology* **32**: 488–497. DOI 10.1089/dna.2013.2070.

Marks PA (2007). Discovery and development of SAHA as an anticancer agent. *Oncogene* **26**: 1351–1356. DOI 10.1038/sj.onc.1210204.

Martinez-Iglesias O, Ruiz-Llorente L, Sanchez-Martinez R, Gracia L, Zambrano A, Aranda A (2008). Histone deacetylase inhibitors: mechanism of action and therapeutic use in cancer. *Clinical and Translational Oncology* **10**: 395–398. DOI 10.1007/s12094-008-0221-x.

Miyazaki T, Kanatani N, Rokutanda S, Yoshida C, Toyosawa S, Nakamura R, Takada S, Komori T (2008). Inhibition of the terminal differentiation of odontoblasts and their transdifferentiation into osteoblasts in Runx2 transgenic mice. *Archives of Histology and Cytology* **71**: 131–146. DOI 10.1679/aohc.71.131.

Mondragón L, Mhaidly R, De Donatis GM, Tosolini M, Dao P, Martin AR, Pons C, Chiche J, Jacquin M, Imbert V, Proïcs E (2019). GAPDH Overexpression in the T Cell Lineage Promotes Angioimmunoblastic T Cell Lymphoma through an NF-κB-Dependent Mechanism. *Cancer Cell* **36**: 268–287.

NCBI Annotation Project (2002). https://www.ncbi.nlm.nih.gov/genome/annotation_euk/process.

Oldberg A, Franzen A, Heinegård D, Pierschbacher M, Ruoslahti E (1988). Identification of a bone sialoprotein receptor in osteosarcoma cells. *Journal of Biological Chemistry* **263**: 19433–19436.

Osathanon T, Ritprajak P, Nowwarote N, Manokawinchoke J, Giachelli C, Pavasant P (2013). Surface-bound orientated Jagged-1 enhances osteogenic differentiation of human periodontal ligament-derived mesenchymal stem cells. *Journal of Biomedical Materials Research Part A* **101A**: 358–367. DOI 10.1002/jbm.a.34332.

Paino F, La Noce M, Tirino V, Naddeo P, Desiderio V, Pirozzi G, De Rosa A, Laino L, Altucci L, Papaccio G (2013). Histone deacetylase inhibition with valproic acid downregulates Osteocalcin gene expression in human dental pulp stem cells and osteoblasts: evidence for HDAc2 involvement. *Stem Cells* **32**: 279–289. DOI 10.1002/stem.1544.

Park JC, Kim JM, Jung IH, Kim JC, Choi SH, Cho KS, Kim CS (2011). Isolation and characterization of human periodontal ligament (PDL) stem cells (PDLSCs) from the inflamed PDL tissue: *in vitro* and *in vivo* evaluations. *Journal of Clinical Periodontology* **38**: 721–731. DOI 10.1111/j.1600-051X.2011.01716.x.

Park JY, Jeon HJ, Kim TY, Lee KY, Park K, Lee ES, Choi JM, Park CG, Jeon SH (2013). Comparative analysis of mesenchymal stem cell surface marker expression for human dental mesenchymal stem cells. *Regenerative Medicine* **8**: 453–466. DOI 10.2217/rme.13.23.

Potdar PD, Jethmalani YD (2015). Human dental pulp stem cells: applications in future regenerative medicine. *World Journal of Stem Cells* **7**: 839. DOI 10.4252/wjsc.v7.i5.839.

Ren D, Wei F, Hu L, Yang S, Wang C, Yuan X (2015). Phosphorylation of Runx2, induced by cyclic mechanical tension via ERK1/2 pathway, contributes to osteodifferentiation of human periodontal ligament fibroblasts. *Journal of Cellular Physiology* **230**: 2426–2436. DOI 10.1002/jcp.24972.

Richon VM (2006). Cancer biology: mechanism of antitumour action of vorinostat (suberoylanilidehydroxamic acid), a novel histone deacetylase inhibitor. *British Journal of Cancer* **95**: S2–S6. DOI 10.1038/sj.bjc.6603463.

Saghiri MA, Asatourian A, Sorenson CM, Sheibani N (2018). Mice dental pulp and periodontal ligament endothelial cells exhibit different proangiogenic properties. *Tissue and Cell* **50**: 31–36. DOI 10.1016/j.tice.2017.11.004.

Sato Y, Ishida S, Motooka H, Takayama K, Tomita Y, Maeda H, Satoh (2001). Decreased bone mass and increased bone turnover with valproate therapy in adults with epilepsy. *Neurology* **57**: 1–3. DOI 10.1212/WNL.57.1.1.

Schroeder TM, Kahler RA, Li X, Westerndorf JJ (2004). Histone deacetylase 3 interacts with Runx2 to repress the Osteocalcin promoter and regulate osteoblast differentiation. *Journal of Biological Chemistry* **279**: 41998–42007. DOI 10.1074/jbc.M403702200.

Seo BM, Miura M, Gronthos S, Bartold PM, Batouli S, Brahim J, Young M, Robey PG, Wang CY, Shi S (2004). Investigation of multipotent postnatal stem cells from human periodontal ligament. *Lancet* **364**: 149–155. DOI 10.1016/S0140-6736(04)16627-0.

Shi L, Cai G, Shi J, Guo Y, Chen D, Chen D, Yang H. (2016). Ossification of the posterior ligament is mediated by osterix via inhibition of the *β*-catenin signaling pathway. *Experimental Cell Research* **349**: 53–59.

Straka M, Straka-Trapezanlidis M, Deglovic J, Vagra I (2015). Periodontitis and osteoporosis. *Neuroendocrinology Letters* **36**: 401–406.

Strausberg RL, Feingold EA, Grouse LH, Derge JG, Klausner RD, Collins FS, Wagner L, Shenmen CM, Schuler GD, Altschul SF, Zeeberg B, Buetow KH, Schaefer CF, Bhat NK, Hopkins RF, Jordan H, Moore T, Max SI, Wang J, Hsieh F, Diatchenko L, Marusina K, Farmer AA, Rubin GM, Hong L, Stapleton M, Soares MB, Bonaldo MF, Casavant TL, Scheetz TE, Brownstein MJ, Usdin TB, Toshiyuki S, Carninci P, Prange C, Raha SS, Loquellano NA, Peters GJ, Abramson RD, Mullahy SJ, Bosak SA, McEwan PJ, McKernan KJ, Malek JA, Gunaratne PH, Richards S, Worley KC, Hale S, Garcia AM, Gay LJ, Hulyk SW, Villalon DK, Muzny DM, Sodergren EJ, Lu X, Gibbs RA, Fahey J, Helton E, Ketteman M, Madan A, Rodrigues S, Sanchez A, Whiting M, Madan A, Young AC, Shevchenko Y, Bouffard GG, Blakesley RW, Touchman JW, Green ED, Dickson MC, Rodriguez AC, Grimwood J, Schmutz J, Myers RM, Butterfield YSN, Krzywinski MI, Skalska U, Smailus DE, Schnerch A, Schein JE, Jones SJM, Marra MA, Mammalian Gene Collection Program Team (2002). Generation and initial analysis of more than 15,000 full-length human and mouse cDNA sequences. *Proceedings of the National Academy of Sciences* **99**: 16899–16903.

Sung IY, Son HN, Ullah I, Bharti D, Park JM, Cho YC, Byun JH, Kang YH, Sung SJ, Kim JW, Rho GJ, Park BW (2016). Cardiomyogenic differentiation of human dental follicle-derived stem cells by suberoylanilide hydroxamic acid and their *in vivo* homing property. *International Journal of Medical Sciences* **13**: 841–852. DOI 10.7150/ijms.16573.

Wang YC, Kong WZ, Xing LH, Yang X (2014). Effects and mechanism of suberoylanilide hydroxamic acid on the proliferation and apoptosis of human hepatoma cell line Bel-7402. *Journal of BUON* **19**: 698–704.

Xia L, Zhang Z, Chen L, Zhang W, Zeng D, Zhang X, Chang J, Jiang X (2011). Proliferation and osteogenic differentiation of human periodontal ligament cells on akermanite and β-TCP bioceramics. *European Cells and Materials* **22**: e82. DOI 10.22203/eCM.v022a06.

Xu Q, Liu Z, Guo L, Liu R, Li R, Chu X, Yang J, Luo J, Chen F, Deng M (2019). Hypoxia mediates runt-related transcription factor 2 expression via induction of vascular endothelial growth factor in periodontal ligament stem cells. *Molecules and Cells* **42**: 763.

Yin L, Cheng W, Qin Z, Yu H, Yu Z, Zhong M, Sun K, Zhang W (2015). Effects of naringin on proliferation and osteogenic differentiation of human periodontal ligament stem cells *in vitro* and *in vivo*. *Stem Cells International* **2015**: 1–9. DOI 10.1155/2015/758706 .

Young MF, Kerr JM, Termine JD, Wewer UM, Wang MG, McBride OW, Fisher LW (1990). cDNA cloning, mRNA distribution and heterogeneity, chromosomal location, and RFLP analysis of human osteopontin (OPN). *Genomics* **7**: 491–502.

Yu Y, Mu J, Fan Z, Lei G, Yan M, Wang S, Tang C, Wang Z, Yu J, Zhang G (2012). Insulin-like growth factor 1 enhances the proliferation and osteogenic differentiation of human periodontal ligament stem cells via ERK and JNK MAPK pathways. *Histochemistry and Cell Biology* **137**: 513–525. DOI 10.1007/s00418-011-0908-x.

Zhao BJ, Liu YH (2014). Simvastatin induces the osteogenic differentiation of human periodontal ligament stem cells. *Fundamental & Clinical Pharmacology* **28**: 583–592. DOI 10.1111/fcp.12050.

Zhu W, Tan Y, Qiu Q, Li X, Huang Z, Fu Y, Liang M (2013). Comparison of the properties of human CD146+ and CD146−periodontal ligament cells in response to stimulation with tumour necrosis factor α. *Archives of Oral Biology* **58**: 1791–1803. DOI 10.1016/j.archoralbio.2013.09.012.